Journal of Alloys and Compounds 509 (2011) 2198–2202

Contents lists available at ScienceDirect

Journal of Alloys and Compounds

journal homepage: www.elsevier.com/locate/jallcom

# Formation of nano quasicrystalline and crystalline phases by mechanical alloying

A.M. Shamah, S. Ibrahim, F.F. Hanna*

*Faculty of Petroleum and Mining Engineering, Suez Canal University, Suez, Egypt*

ARTICLE INFO

*Article history:*
Received 26 June 2009
Received in revised form 31 October 2010
Accepted 2 November 2010
Available online 10 November 2010

*Keywords:*
Nano quasicrystalline
$Al_{62.5}Cu_{25}Fe_{12.5}$
Mechanical alloying
Rapid solidification
X-ray diffraction

ABSTRACT

In the present work, the formation of nano quasicrystalline icosahedral phase in $Al_{86}Cr_{14}$, $Al_{84}Fe_{16}$ and $Al_{62.5}Cu_{25}Fe_{12.5}$ alloys has been investigated by mechanical alloying. Mixtures of quasicrystalline and related crystalline phases have been observed under various milling conditions. The X-ray diffraction, differential thermal analysis and electrical resistivity techniques have been used for characterization and physical property measurements. The particle size was calculated by X-ray profile using Williamson–Hall plot method and it was found to be 25–50 nm size.



## 1. Introduction

A nanomaterial of the icosahedral phase has been the object of the quick growing attention in the last few years due to its potential application in various fields (e.g. vehicles industry). These materials are known to exhibit an unusual combination of properties such as strength, good ductility, high fracture toughness, and good corrosion resistance [1]. These new and unsuspected physical properties are not found in natural materials [2]. Recently, the production of amorphous, intermetallic, quasi-crystalline, and nanocrystalline materials has received much attention. These materials can be obtained by non-equilibrium processes, such as mechanical alloying (MA), rapid solidification (RS), vapor phase condensation, or irradiation/ion implantation. MA is a simple and adaptable process that transfers high amount of energy from milling balls to the alloy powder during the milling process [3]. MA is a dry solid-state powder processing technique involving repeated welding, fracturing and re-welding of powder particle in a high-energy ball mill. The main attributes of MA are the extension of a solid solution, refinement of structures in the nanometer range, production of fine dispersion of a second phase, and synthesis of novel crystalline, quasi-crystalline and amorphous phases.

There is an increasing interest in the development of high-strength light alloys because of the recent strong demand for weight reduction in transportation vehicles. So, aluminum alloys are the most widely used light alloys for weight reduction in structural components [4–6] and low coefficient of friction and high resistance to corrosion [7]. It is found that the nano quasicrystalline aluminum iron alloy exhibited intermediate strength and ductility values at room temperature among the alloys studied and showed better microstructure stability at high temperature [8].

However, further strengthening may be possible by grain refinement down to the nanocrystalline range. One way to achieve the nanocrystalline and nano quasicrystalline microstructure from aluminum-based alloy is the rapid solidification process and mechanical alloying.

Al–Cr system is known to form icosahedral quasicrystal by rapid solidification [9–13] or by using MA technique [14] over a wide composition range. However, different reported results appear to be processing condition dependence. Considerable amount of work has also been concentrated on the synthesis of Al–Fe systems by MA, where both quasi and amorphous phases' formation are possible [15,16]. The sequences of phases which appear following milling or milling with thermal treatment are in contradiction in their results (see [17–19]).

On the other hand, the rapid solidification is considered to be one of the most important methods for producing the quasicrystalline phase. Earlier studies concerning the production of quasicrystalline phase indicated that, it is possible to obtain a pure quasicrystalline phase, i-phase, in AlCuFe by rapid solidification followed by annealing at 800 °C [20,21]. The as quenched sample contains a small amount of cubic β-AlFe phase and a considerable amount of structural defects, which are both eliminated by the subsequent annealing treatment [22]. However, in the rapidly quenched $Al_{61}Cu_{26}Fe_{13}$ there was orientation relationship found between the lattice of i-phase and the β-solid solution, where β-solid solution contains fine regions of ω-like displacement [23]. Moreover, mechanical alloying and subsequent heat treatment pro-

* Corresponding author. Tel.: +20 101843720; fax: +20 623360257.
*E-mail address:* fariedhanna@yahoo.com (F.F. Hanna).

0925-8388/$ – see front matter © 2010 Elsevier B.V. All rights reserved.
doi:10.1016/j.jallcom.2010.11.001

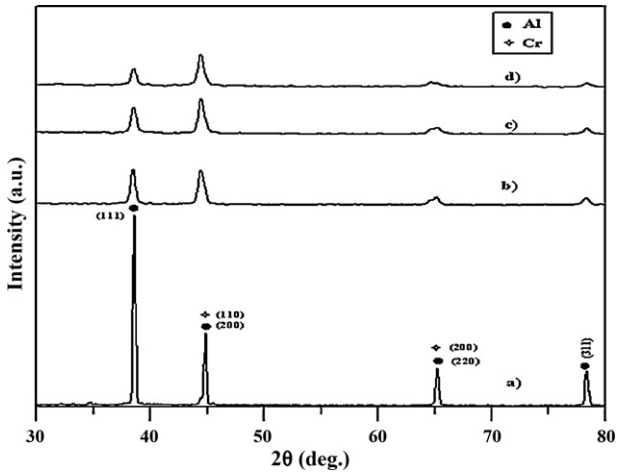


**Fig. 1.** XRD patterns of mechanically $Al_{86}Cr_{14}$ for: (a) 0 h, (b) 20 h, (c) 40 h, and (d) 60 h.

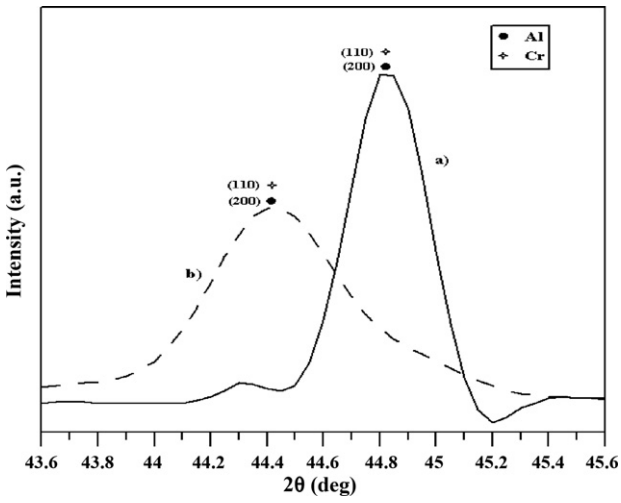


**Fig. 2.** The relationship between the peaks shift versus the intensity for Al and Cr elements at different milling times.

cesses were reported to enhance the formation of quasicrystalline phase for another ternary alloyed systems [24–26].

In this work, XRD technique was used to study the effects of the mechanical alloying MA processes and the subsequent thermal treatments on the formation of quasicrystals in AlCr and AlFe systems. A further investigation on the effect of a combination between rapid solidified and mechanical alloying techniques are used to enhance the i-phase formation in the ternary AlCuFe system with a specific composition which was done.

## 2. Experimental details

Pure aluminum (99.95%), iron (97.7%), and chromium (98%) are used as starting powders, and a 2 wt% to organic surfactant (stearic acid) is added to the powders during milling as a process control agent. Two nominal mixtures of Al–14 at.% Cr and Al–16 at.% Fe are used. The attritor vial is used for milling and the ball to powders weight rate of 10:1 with milling speed of 500 rpm. To minimize contamination with oxygen and/or nitrogen, the mechanical alloying process is carried out under a continuous dry argon atmosphere.

A sample of nominal composition $Al_{62.5}Cu_{25}Fe_{12.5}$ was prepared by rapid solidification of the melt. Commercial iron, electrical copper, and an $AlCu_{25}$ master alloy of purity 99.9% were used for alloying. The melt was rapidly solidified by projecting it into twin rolls system which consists of two pure copper cylinders with rotational speed 1400 rpm. Thin ribbons of dimensions ≈0.25 mm × 4 mm × 15 mm were obtained.

15 g of rapid solidification sample followed by annealing at 800 °C for 1 h was grinded and placed in attritor with 150 g balls of different sizes. The milling process was performed for 10 h, 15 h and 20 h.

The thermal stability was examined using a Perkin-Elmer DTA, with a constant heating rate of 15 °C/s in ambient air. The produced phases in all samples are characterized by XRD, using Siemens D5000 diffractometer with copper Kα radiation, λ = 0.15406 nm and nickel filter. The diffractometer was operated with step time one second and step size 0.05° as a continuous mode. The electrical resistivity of the as quenched and annealed samples, and its dependence with temperature was measured by the four-probe method.

## 3. Results and discussion

### 3.1. Mechanical alloyed of $Al_{86}Cr_{14}$

X-ray diffraction patterns (XRD) of Al–14 at.% Cr powder after milling for various intervals of time are shown in Fig. 1. It is generally observed that both peak intensities of aluminum and chromium elements decrease with increasing processes time, up to 60 h. This could indicate that there is no alloying taking place and amorphization could be expected at higher milling times which depend on the milling intensity.

The observed small shift of peaks positions in XRD patterns, Fig. 2, could be related to a formation of super saturation solid solution phase of Cr in Al. Williamson–Hall plot method [27] is carried out in order to determine both crystallite size and strain. A minimum of 25 nm crystallite size and 0.067 strains were reached after 40 h milling (Table 1). Two exothermic peaks at 372 and 582 °C are observed while heating the milled powder up to 600 °C (Fig. 3a). The first peak could be related to annealing out of the defects generated during the milling process. The second one may be due to the formation of a precipitate phase from the supersaturated solid solution.

**Table 1**
Crystallite size and strain variations with milling time for "$Al_{86}Cr_{14}$".

| Milling time | Particle size (nm) | Strain |
|---|---|---|
| 10 | 69.3 | 0.018 |
| 20 | 39.2 | 0.029 |
| 30 | 31.4 | 0.044 |
| 40 | 24.6 | 0.069 |
| 50 | 25.2 | 0.068 |
| 60 | 25.9 | 0.064 |

Based on the thermal analysis results, various intervals of annealing times ranging from 30 min to 6 h are carried at 590 °C for the 40 h milled powder. Fig. 4 shows XRD results of the annealed powder. Phase formation readily observed and appears to be a rather time dependent.

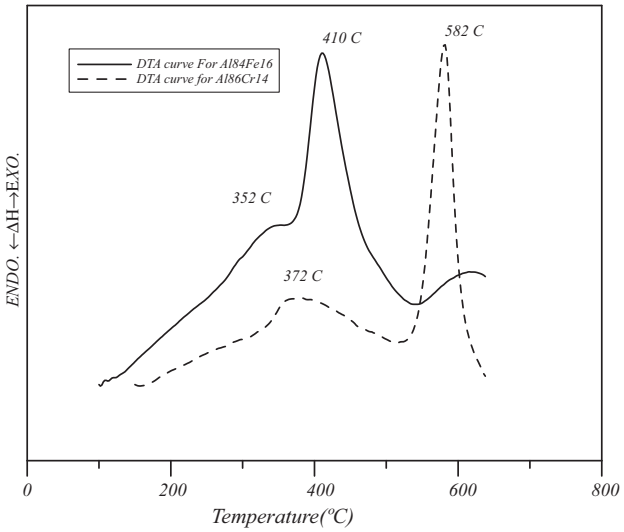


**Fig. 3.** DTA curves of 40 h milled powder for (a) $Al_{86}Cr_{14}$ and (b) $Al_{86}Fe_{14}$.

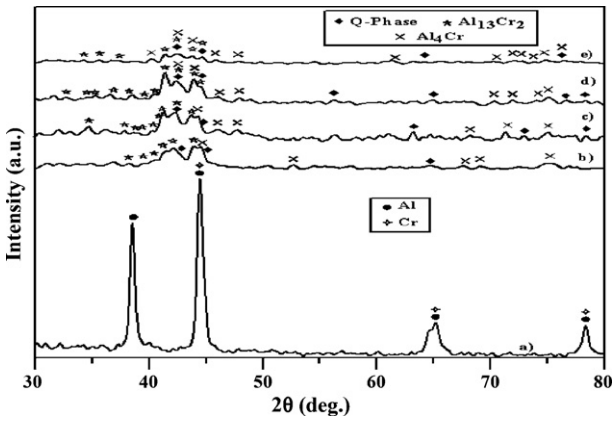


**Fig. 4.** XRD patterns for 40 h mechanically alloyed $Al_{86}Cr_{14}$ annealed at 590 °C for (a) as milled, (b) 30 min, (c) 2 h, (d) 4 h, and (e) 6 h.

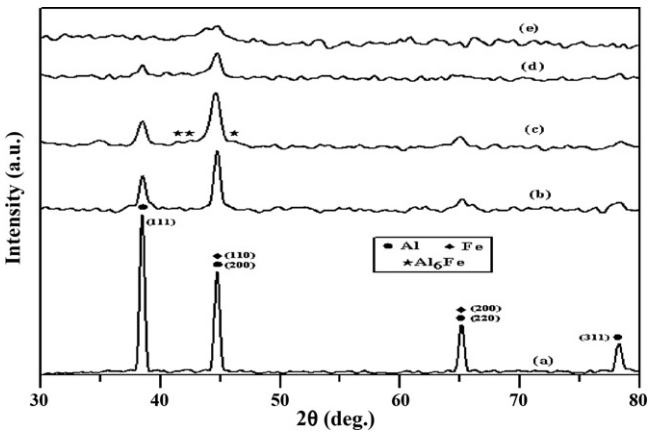


**Fig. 5.** XRD patterns of mechanically alloyed $Al_{84}Fe_{16}$ for (a) 0 h, b) 20 h, c) 40 h, d) 60 h, e) 190 h.

The quasicrystalline phase was identified in the XRD after 30 min isothermal annealing and continues to increase in quantity up to 4 h annealing after which it decreases. The annealed structure contains two other phases, the first one can be indexed as $Al_4Cr$ hexagonal type, using reported *d*-values of this phase which is known to be isomorphous with μ-$Al_4Mn$ [28], therefore it is called μ-$Al_4Cr$ type. This phase had been reported to form in the as quenched and rapidly solidified Al–Cr alloys with composition up to 20 at.% Cr [13,29]. It has been reported that for a rapidly solidified Al–Cr system in the Al-rich side, it is possible to obtain additional two other phases ξ-$Al_4Cr$ and ξ′-$Al_4Cr$ and they are closely related to μ-$Al_4Cr$ phase type and both are an approximation of the icosahedral phase [13].

Moreover, results also showed the possible existence of a third phase of the type $Al_{13}Cr_2$ in the annealed material, this phase is also reported [12] to coexist with icosahedral rapidly quenched Al–Cr, and both phases (quasi and intermetallic $Al_{13}Cr_2$) seemed to be more or less stable compared to $Al_4Cr$. It is to be noted that the present results agreed to a large extent with similar work on Al–Cr processed by mechanical alloying. It is worthy to mention that a planetary ball milling for 60 h followed by heating at 300 °C for 100 h and almost single icosahedral phase is obtained for the $Al_{86}Cr_{14}$ composition [30]. In that case, milling conditions difference can be responsible for such results, mainly the high intensity of planetary ball milling, other factors such as milling speed, initial material purity and contamination can also be responsible for the difference in the reported results. The complex structures obtained following the present condition of processing resemble the one for Al–Cr alloys produced by rapid solidification [13,29].

It is expected that the quasiphase will occur on α-Al (Cr) supersaturated phase enriched in chromium which is formed during milling, while the second phases $Al_4Cr$ and $Al_{13}Cr_2$ are expected to be formed due to the interaction between the remaining Al and Cr elements during milling.

### 3.2. Mechanical alloyed of $Al_{84}Fe_{16}$

XRD patterns of Al with 16 at.% Fe after various processing times are shown in Fig. 5. Again, increasing milling time causes the peaks to be broadening and decrease its intensity. The peak broadening is a result of reducing particle size and introducing strain during milling. The calculated crystallite size and strain are ≈37 nm and ≈0.072 after 40 h milling respectively as indicated in Al–Cr system. Furthermore, Al-lines shift slightly toward higher angles suggested alloying of Fe with Al leading to a solid solution formation, similar to that in Al–Cr system. However, a few new low intensities peaks mainly in the low angle region of $2\theta = 38–44^\circ$ appeared in XRD pattern after 40 h milling and continue up to 60 h milling. Those lines could be indexed as a metastable $Al_6Fe$ phase. However, a fewer number of peaks are present and makes it difficult to evaluate the *d*-values change with further milling at 60 h. On the other hand, it is not likely that the metastable $Al_6Fe$ will transform to the rather stable $Al_3Fe$ phase with further milling. Hence, $Al_3Fe$ phase has a complex monoclinic structure with a large unit cell, where a higher atomic mobility is needed and is not likely to be provided by milling process under the present conditions. Moreover, only partial amorphization is observed after milling for 190 h as shown in Fig. 5. It is possible that with increasing milling that amorphization would be completed.

A differential thermal analysis study of the MA powder indicated the presence of two exothermic peaks at 352 and 410 °C (Fig. 3b). Isothermal heating for various time intervals is carried therefore at 500 °C on the 40 h milled specimens in order to examine the possible phase evolution during annealing. XRD results indicated changes mainly in the metastable $Al_6Fe$ phase lines leading to the formation of both $Al_{13}Fe_4$ and $Al_3Fe$, through the interaction with the elemental lines of α-Al and α-Fe (Fig. 6). The melt spun technique confirmed the presence of various metastable phases among which is the $Al_{13}Fe_4$ with alloys up to 20% Fe [31]. However, in comparison with less iron-content alloy ≈12 at.% Fe only $Al_3Fe$ is

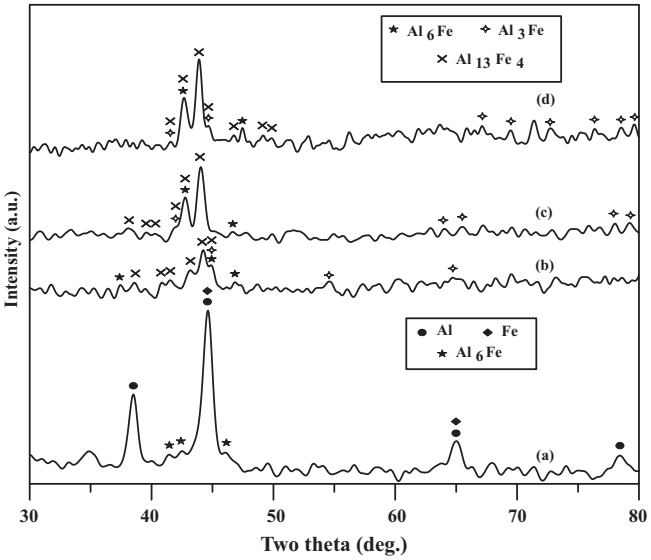


**Fig. 6.** XRD patterns for 40 h mechanically alloyed $Al_{84}Fe_{16}$ annealed at 500 °C for (a) as milled, (b) 30 min, (c) 2 h, and (d) 4 h.

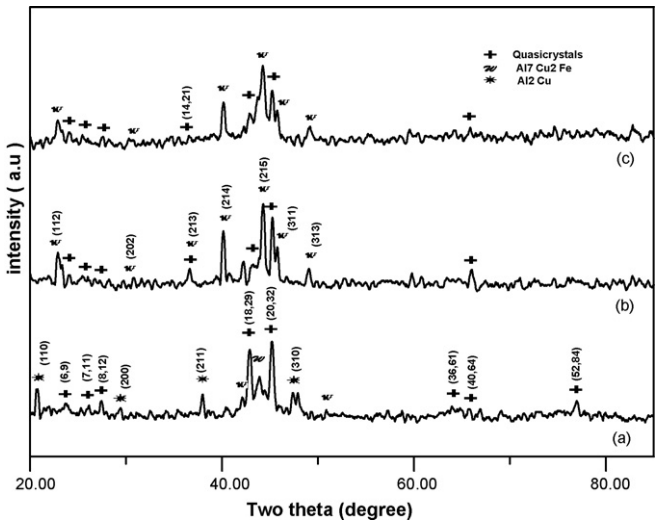


**Fig. 7.** XRD patterns of $Al_{62.5}Cu_{25}Fe_{12.5}$: (a) as quenched, (b) annealed at 680 °C for 1 h, and (c) annealed at 800 C for 1 h.

formed following both mechanical alloying and thermal treatment [16]. It is to be noted that $Al_6Fe$ lines are still observed even after 4 h annealing, i.e. the dissolution or rather the transformation process has a slow-rate. Different sequences of phase transformation have been given by several authors [15,32], from which it is possible to show that the initial processing conditions and annealing temperature, control to large extent the final structure produced by milling and subsequent annealing treatment.

### 3.3. The ternary $Al_{62.5}Cu_{25}Fe_{12.5}$ prepared by rapid solidification

A rapid solidification technique is used to produce the quasicrystalline phase in the ternary $Al_{62.5}Cu_{25}Fe_{12.5}$ alloy composition. However, a single quasicrystalline phase was not obtained, but the produced ribbons consist of three mixtures of phases (Fig. 7). This could be possible due to the rate of cooling was not high enough. Moreover, thermal stability tests indicated the presence of single exothermic peak at 670 °C, as shown in Fig. 8. Therefore, annealing was carried at two temperatures of 680 and 800 °C for further thermal stability assessment.

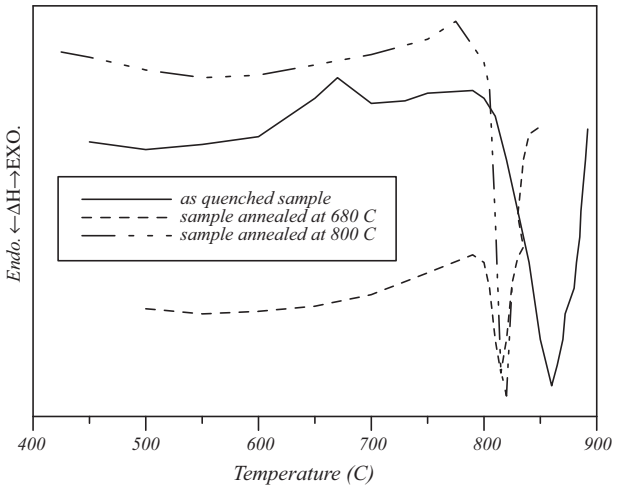


**Fig. 8.** DTA curve of the as quenched sample $Al_{62.5}Cu_{25}Fe_{12.5}$, annealed at 680 °C and 800 °C for 1 h.

#### 3.3.1. The rapid solidified structure

The obtained ribbons XRD, Fig. 7a shows that a quasicrystalline (i-phase) is presented in a relative high volume fraction, in addition to two other phases that are most likely to be $Al_2Cu$ phase and $Al_7Cu_2Fe$ (ω-phase). The fact that under present rapid solidification that more than one phase appears, indicate that the quasi-phase formation is processing dependent.

The electrical resistivity of the sample is measured at room temperature giving a resistivity value of 625 μΩ cm, which is mainly related to the presence of the icosahedral AlCuFe phase. The pure iscosahedral is reported to give a value resistivity of 1000 μΩ cm [33]. The temperature dependence of resistivity from 20 K up to room temperature is shown in Fig. 9, the electric resistivity is observed to increases linearly up to room temperature which is the usual behavior of the ordinary metals and not to quasi-phase. The resistivity ratio $\rho_{20}/\rho_{295}$ for the present as-quenched material is 0.42. However, it is in the order of 2.0 for a simple phase quasicrystalline and about 0.1 or less for metallic alloys. Therefore, the present ratio can form the behavior of phases mixture of the as-quenched material.

#### 3.3.2. Structure at 680 °C

Following the XRD pattern of the sample annealed at 680 °C for 1 h as shown in Fig. 7b, it is observed that after this treatment, the $Al_2Cu$ phase disappeared completely, and the amount of the $Al_7Cu_2Fe$ phase increased to a large extent. The results indicate that the instability nature of this phase ($Al_2Cu$) by which it might dissolve and transform to the more stable $Al_7Cu_2Fe$ phase as reported in [34].

The DTA curve of the sample after annealing at 680 °C shown in Fig. 8 indicates that, there is no further possible phase transformation to be expected. Measurements of the electrical resistivity at room temperature of the sample annealed at 680 °C give the value of 460 μΩ cm. This value is less than the value obtained for the as-quenched sample, which could be due to the dissolution of the $Al_2Cu$ phase and the increasing of the volume fraction of the ω phase.

#### 3.3.3. Structure at 800 °C

The X-ray diffraction pattern and DTA measurement, of the annealed sample at 800 °C, are shown in Figs. 7c and 8 respectively. The obtained data showed a similar structure and behavior to the one obtained after 680 °C annealing, i.e. the structures are stable between 680 and 800 °C. This result is in analogous with the electrical resistivity measurements at room temperature, 470 μΩ cm. The temperature dependence of the resistivity measurement for the annealed sample at 800 °C, Fig. 9, showed that the resistivity increases as the temperature increases. That is an indication for metallic behavior contribution, i.e. further phase transformations are not expected.

### 3.4. The effect of mechanical milling on rapid solidification structure

To study the effect of mechanical alloying on a rapid solidified sample, various milling times were done on that sample after the thermal treatment at 800 °C. The XRD patterns of the various milled samples are shown in Fig. 10. The patterns show that, with the increase of the milling time, the peaks of the ω phase ($Al_7Cu_2Fe$) decrease in their intensity and also in their number, and disappear completely after 15 h of milling. On the other hand, with increasing the milling time, the icosahedral phase is still presented in an appreciable volume fraction, in a way that, it may be thought that the process of milling tends to enhance the i-phase formation. However, further work should be carried out in order to determine the exact volume fraction of i-phase after milling process. It is also to be

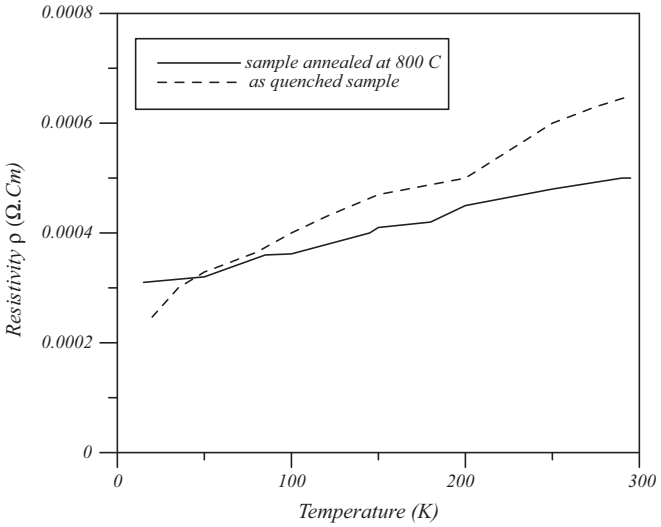


**Fig. 9.** Variation of electrical resistivity with temperature for the as quenched sample and that annealed at 800 °C.

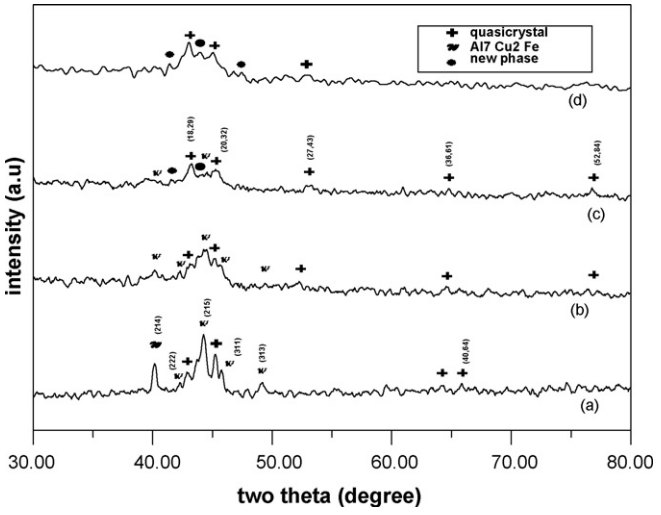


**Fig. 10.** X-ray diffraction pattern of Al–Cu–Fe alloyed sample prepared by rapid solidification followed by annealing at 800 °C. (a) Before milling, (b) after 5 h milling, (c) after 10 h milling, and (d) after 15 h milling.

noted that, the peaks of the i-phase are broadened with the increase of the milling time, which is expected due to the mechanical straining present during the process of milling [35]. A new undefined phase began to appear after 10 h of milling and this phase continues to increase with further milling but there are not enough lines to be indexed. However, other routes were used to produce the icosahedral quasicrystalline phase in AlCuFe through mechanical alloying and annealing sequence [36], the main phases obtained compare well with the present processing sequence.

## 4. Conclusions

MA and subsequent heat treatment of $Al_{86}Cr_{14}$, led to the formation of quasicrystalline phase in addition to other two crystalline phases $Al_{13}Cr_2$ and $Al_4Cr$. On the other hand, MA and subsequent heat treatment of $Al_{84}Fe_{16}$, led to the formation of stable $Al_3Fe$ and $Al_{13}Fe_4$ phases, besides the metastable $Al_6Fe$ phase. In both compositions nanocrystalline powders particle of ≈25 nm and ≈37 nm size have been obtained for $Al_{86}Cr_{14}$ and $Al_{84}Fe_{16}$ respectively.

It is possible to obtain a quasicrystalline phase $Al_{62.5}Cu_{25}Fe_{12.5}$ (i-phase) by rapid solidification technique under the present conditions, but not as a single phase even after annealing. Instead, two phases were obtained after annealing (i-phase + ω phase). Such deviation could well be related to slow rate of cooling lead to certain composition separation. This deviation can be due to some material losses during the process of alloy melting. Thermal analysis of the annealed structure proves its stability up to melting temperature. Addition milling to rapid solidification structure did not lead to massive transformation to i-phase.

## References

[1] C. Suryanarayana, Non-equilibrium Processing of Materials, Pergamon Materials Series, vol. 2, 1999.
[2] T. Tsong, Mater. Sci. Eng. A 286 (2000) 87.
[3] C. Suryanarayana, Prog. Mater. Sci. 46 (2001) 1–184.
[4] T.T. Sasaki, T. Ohkubo, K. Hono, Acta Mater. 57 (2009) 3529–3538.
[5] M. Galano, F. Audebert, A. Garcia, I.C. Stone, B. Cantor, J. Alloys Compd. 495 (2010) 372–376.
[6] E. Huttunen-Saarvirta, J. Alloys Compd. 363 (2004) 150–174.
[7] E. Huttunen-Saarivirta, T. Tiainen, Mater. Chem. Phys. 85 (2004) 383–395.
[8] A. Inoue, Prog. Mater. Sci. 43 (1996) 365.
[9] A. Inoue, H. Kimura, T. Masumoto, J. Mater. Sci. 22 (1987) 1758–1768.
[10] K.F. Kobayashi, N. Tachibana, P.H. Shingu, J. Mater. Sci. 24 (1989) 2437–2443.
[11] D.W. Lawther, D.J. Liod, R.A. Dunlap, Mater. Sci. Eng. A 123 (1990) 33–38.
[12] C. Zhenhua, W. Yun, Z. Duosan, J. Xingyang, Scripta Metall. Mater. 24 (1990) 599–604.
[13] K.Y. Wen, Y.L. Chen, K.H. Kuo, Metall. Trans. A 23 (1992) 1445–2437.
[14] M.S. Archana, N. Hebalkar, K. Radha, J. Joardar, J. Alloys Compd. 501 (2010) 18–24.
[15] V.I. Fadeeva, A.V. Lenov, Mater. Sci. Eng. A 206 (1996) 90–94.
[16] M.A. Morris, D.G. Morris, Mater. Sci. Eng. A 136 (1991) 59–70.
[17] F. Cardellini, V. Contini, R. Gupta, G. Mazzone, A. Motone, A. Perin, G. Principi, J. Mater. Sci. 33 (1998) 2519.
[18] F. Zhou, R. Lück, K. Lu, M. Rühle, Z. Mettalkd. 92 (7) (2001) 675–681.
[19] L. D'Angelo, L. D'Onofiro, G. Gonzalez, J. Alloys Compd. 483 (2009) 154–158.
[20] Y. Calvayrac, A. Quivy, M. Bessiere, S. Lefebvre, M. Quiquandon, D. Gratias, J. Phys. France 51 (1991) 417.
[21] J. Davaud Rzepski, A. Quivy, Y. Calpvayrac, M. Quiquandon, D. Gratias, Philos. Magn. B 60 (1989) 855.
[22] Y. Calvayrac, Journal de Physique, Colloque2, Supplement auj De Phys 6 (1996).
[23] E.V. Shalaeva, J. Alloys Compd. 342 (2010) 134–138.
[24] P. Barua, B.S. Murty, B.K. Mathur, V. Srinivas, J. Appl. Phys. 91 (8) (2002) 5353.
[25] T.P. Yadav, N.K. Mukhopadhyay, R.S. Tiwari, O.N. Srivastava, Philos. Magn. 87 (2007) 3117–3125.
[26] T.P. Yadav, N.K. Mukhopadhyay, R.S. Tiwari, O.N. Srivastava, Philos. Magn. Lett. 87 (2007) 781–789.
[27] B.D. Cullity, S.R. Stock, Elements of X-ray Diffraction, third edition, Prentice-Hall, New Jersy, USA, 2001, pp. 399–402.
[28] M. Palm, J. Alloys Compd. 252 (1997) 192.
[29] M.A. Marcus, V. Elser, Philos. Magn. 54 (1986) 101.
[30] J. Eckert, L. Schultz, K. Urban, Acta Metall. Mater. 39 (7) (1991) 1497–1506.
[31] D.H. Kim, B. Cantor, Philos. Magn. A 69 (1) (1994) 45–55.
[32] D.K. Mukhopadhyay, C. Suryanarayana, F.H. Sam Froes, Metall. Mater. Trans. 26A (1995) 1939–1946.
[33] X. Yong, I.T. Chang, I.P. Jones, J. Alloys Compd. 387 (2005) 128.
[34] S.D. Kaloshkin, N. Tcherdyntsev, A.I. VLaptev, A.A. Stepashkin, E.A. Afonina, A.L. Pomadchik, V.I. Bugakov, J. Mater. Sci. 39 (2004) 5399.
[35] R.S. Tiwari, T.P. Yadav, N.K. Mukhopadhyay, M.A. Shaz, O.N. Srivastava, Z. Kristoll. 224 (2009) 26.
[36] S. Yin, Z. Xie, Q. Bian, B. He, Z. Pan, Z. Sun, Z. Wei, L. Qian, S. Wei, J. Alloys Compd. 455 (2008) 314–321.